THE PUBLISHING HOUSE
OF THE ROMANIAN ACADEMY

PROCEEDINGS OF THE ROMANIAN ACADEMY, Series A,
Volume 20, Number 1/2018, pp. 87–95

CONDITION MONITORING OF VEHICLE DAMPERS USING SHOCK EXCITATION

Tudor SIRETEANU [1], Ana-Maria MITU [1], Adrian Ioan NICULESCU [1], Miroslav KOWALSKI [2], Antoni JANKOWSKI [3]

[1] Institute of Solid Mechanics of the Romanian Academy, 15 Constantin Mille St., 70701, Bucharest, Romania
[2]Air Force Institute of Technology, Poland, [3] Institute of Aviation, Poland
Corresponding author: Ana-Maria MITU, E-mail: anamariamitu@yahoo.com

Abstract. In this paper is developed a condition monitoring method for the dampers of road vehicles suspension and airplanes landing gear. The method is based *on phase difference of free* vertical accelerations recorded simultaneously on sprung mass and unsprung mass for shock inputs applied to area of contact between the ground and the tire. By using the quarter car model and suitable band pass filtering of recorded signals, an analytical relation between the phase shift and the condition of suspension dampers measured by the linear equivalent damping ratio is assessed for different types of applied shock inputs. It is shown that this parameter is almost independent of different factors that can change the visco-elastic damping properties of tires including temperature, pressure and wheel loads. The method is also applied to viscous nonlinear damping characteristics by using a linearization method based on the equality of dissipated power per cycle and the corresponding values of damping efficiency index.

Key words: vehicle suspensions, shock inputs, dampers condition monitoring, damping efficiency index.

1. INTRODUCTION

Vibration-based condition monitoring techniques have found application in many branches of engineering due to high availability of measuring devices (e.g. accelerometers, data acquisition units, dedicated software, etc.) and the advancement of signal processing methods. However, there are still difficulties in proper condition assessment of certain engineering structures, which arise from the nature of their dynamic behavior and phenomena associated with their operation. This kind of obstacles is particularly apparent in the case vehicle's suspension monitoring. The suspension plays a major role in vehicle dynamics being crucial system for both ride comfort and road holding/handling. The condition of suspension dampers is very important for ensuring an optimum compromise between these two contradictory criteria [1], [2]. Therefore, it is necessary to check their condition regularly in order to assess an effective predictive maintenance strategy. Usually, this is done by using special rigs to measure their damping efficiency. The tests procedures can require or not the removal of dampers from the vehicle suspension. A more convenient procedure to achieve this goal is based on vibration measurement conducted on vehicles in operating conditions. Mostly, these types of condition monitoring techniques have been recently developed for railway vehicles [3-10] and can be classified in two categories: and model-less methods. In this paper is proposed a model-based method for vehicle suspension dampers, based on acceleration measurements of sprung and unsprung masses for shock inputs. The method addresses the road vehicle suspensions and airplanes landing gears.

2. ANALYTICAL MODEL

The schematic of mechanical model utilized in this paper to assess the damping capacity of the shock absorbers used in vehicle suspensions is shown in Fig. 1, where:

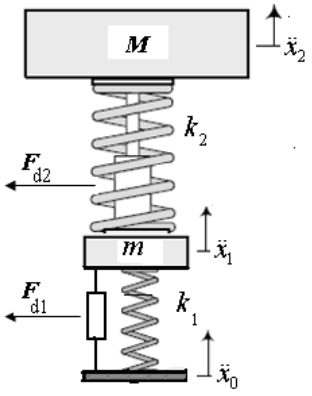

Fig. 1 – Quarter car model of vehicle suspension .

m, M – unsprung and sprung masses distributed on one wheel or one axle;
k_1, F_{d1} – tire stiffness and damping characteristics;
k_2, F_{d2} – stiffness and damping characteristics of vehicle suspension;
$\ddot{x}_0(t)$ – acceleration of shock input;
$\ddot{x}_1(t), \ddot{x}_2(t)$ – accelerations of unsprung and sprung masses, measured simultaneously on the same vertical axis.

The system equations of motion are

$$\begin{cases} m\ddot{x}_1 = -F_{d1} - k_1(x_1 - x_0) + F_{d2} + k_2(x_2 - x_1) \\ M\ddot{x}_2 = -F_{d2} - k_2(x_2 - x_1). \end{cases} \tag{1}$$

In order to use the shock acceleration $\ddot{x}_0(t)$ as the input of system (1), the following variables are introduced:

$$y_1 = x_1 - x_0,\ \ddot{x}_1 = \ddot{y}_1 + \ddot{x}_0,\ y_2 = x_2 - x_1,\ \ddot{x}_2 = \ddot{y}_2 + \ddot{x}_1 = \ddot{y}_2 + \ddot{y}_1 + \ddot{x}_0. \tag{2}$$

The equations of motion (1) can be rewritten as

$$\begin{cases} \ddot{y}_1 = -f_1(y_1, \dot{y}_1) - \omega_1^2 y_1 + \mu f_2(y_2, \dot{y}_2) + \mu\omega_2^2 y_2 - \ddot{x}_0 \\ \ddot{y}_2 = f_1(y_1, \dot{y}_1) + \omega_1^2 y_1 - (1+\mu) f_2(y_2, \dot{y}_2) - (1+\mu)\omega_2^2 y_2 \end{cases} \tag{3}$$

where

$$\omega_1 = \sqrt{\frac{k_1}{m}},\ f_1(y_1, \dot{y}_1) = \frac{F_{d1}(y_1, \dot{y}_1)}{m},\ \omega_2 = \sqrt{\frac{k_2}{M}},\ f_2(y_2, \dot{y}_2) = \frac{F_{d2}(y_2, \dot{y}_2)}{M},\ \mu = \frac{M}{m},\ \frac{k_2}{m} = \mu\omega_2^2. \tag{4}$$

In general, the functions $f_i(y_i, \dot{y}_i),\ i = 1,2$ are described by nonlinear expressions of the relative displacement and velocity. In order to represent dissipative characteristics, these functions must have the same sign as the relative velocity, i.e. $f_i(y_i, \dot{y}_i)\,\dot{y}_i \geq 0,\ i = 1,2$. Usually, the suspension damping characteristics are obtained by measuring the developed force $F_{d2}(y, \dot{y})$ for harmonic relative motions $y(t) = Y \sin \omega t$, imposed between the mounting points of tested dampers. In most data sheets provided by the manufactures are specified only the intervals of force values that should be developed by vehicle dampers for specified values of relative velocity to be considered in good condition. The procedure proposed in this paper for assessing the dampers condition is based on the modification of average phase shift between the measured accelerations of unsprung and sprung masses for shock acceleration input, predicted by using the quarter car model shown in Fig. 1. This testing method is less costly and much simpler to be applied for most types of vehicle suspensions than the currently employed testing procedures which require specialized equipment. For road vehicles the riding over a conveniently profiled bump can provide the desired shock acceleration input, while for airplanes this type of input is provided by the landing itself [11]. It should be mention that the recorded hydraulic characteristics display a certain hysteresis behavior. The main causes of this phenomenon are discussed in [12], where an averaged graph of points of hysteresis loops $F_{d2}(y, \dot{y})$ corresponding to maximum linear velocities $\dot{y}_{max} = \omega Y$ of successive imposed cyclic motions with constant amplitude and different frequencies (for both compression and rebound strokes) is

assumed to be representative for the hydraulic characteristic $F_{\mathrm{d2}}(\dot{y})$. For a large class of hydraulic shock absorbers types this can be described analytically by a viscous power law of the form [13]:

$$F_{\mathrm{d2}}(\dot{y}) = a_2 |\dot{y}|^{\alpha} \operatorname{sgn} \dot{y}, \quad a_2, \alpha > 0. \tag{5}$$

The dissipated power for an imposed harmonic motion with maximum velocity $\dot{y}_{\max}$ is given by

$$P_{\mathrm{d2}}(\dot{y}_{\max}) = \int_{-\dot{y}_{\max}}^{\dot{y}_{\max}} \left| F_{\mathrm{d2}}(\dot{y}) \right| \mathrm{d}\dot{y} = 2a_2 \frac{\dot{y}_{\max}^{\alpha+1}}{\alpha+1}. \tag{6}$$

The linear viscous damping characteristic and the dissipated power per cycle is obtained from (6) for $a_2 = c_2$, $\alpha = 1$:

$$F_{\mathrm{d2}}(\dot{y}) = c_2 \dot{y}, \; P_{\mathrm{d2}}(\dot{y}_{\max}) = c_2 \dot{y}_{\max}^2. \tag{7}$$

By equating the dissipated powers given in (6) and (7) yields an energetic correspondence between the coefficients of nonlinear and linear viscous damping characteristics (5) and (7), for a chosen value of $\dot{y}_{\max}$:

$$a_2 = \frac{\alpha+1}{2\dot{y}_{\max}^{\alpha-1}} c_2. \tag{8}$$

In Figs. 2 and 3 are shown the plots of damping characteristics (5) for different values of exponent α which provide the same dissipated power $P_{\mathrm{d2}}(\dot{y}_{\max}) = 1100$ W for $\dot{y}_{\max} = 1$ m/s as with the linear damping characteristic obtained for $\alpha = 1, c_2 = 1100$ Nm^{-1}s .

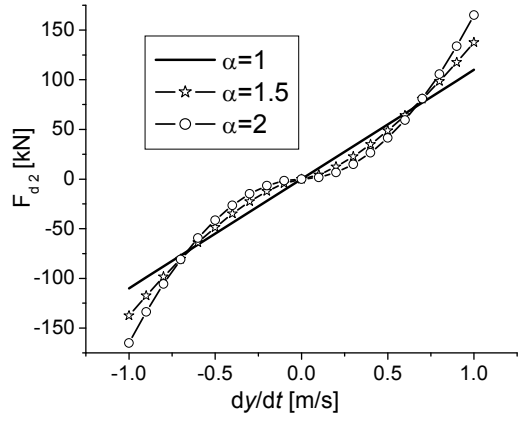

Fig. 2 – Nonlinear and equivalent linear damping characteristics obtained for $\alpha \geq 1$.

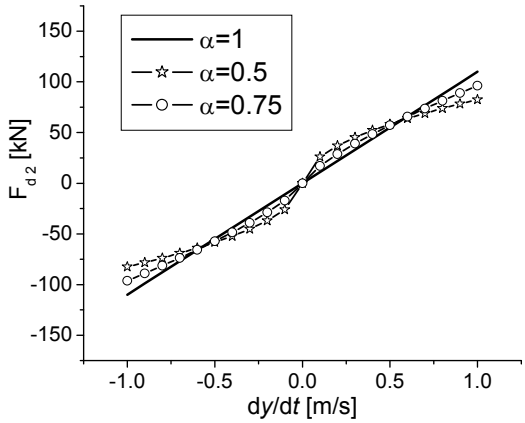

Fig. 3 – Nonlinear and equivalent linear damping characteristics obtained for $0 < \alpha \leq 1$.

3. MODELING THE SHOCK ACCELERATION INPUT

A large category of acceleration time histories recorded for shock tests can be approximated with good accuracy by analytical expressions having the following form

$$\ddot{x}_0(t) = A_0 + \frac{V_0}{\sigma\sqrt{2\pi}} \exp\left[-\frac{(t-t_{\mathrm{c}})^2}{2\sigma^2} \right] = A_0 + V_0 p(t; t_{\mathrm{c}}, \sigma) \tag{9}$$

where $p(t;t_c,\tau)$ is the Gaussian distribution density function with mean t_c and variance σ. In Figs. 4 and 5 are presented the time histories of acceleration measured for drop tests of a rigid mass on different elastomeric materials in order to assess their shock absorbing properties.

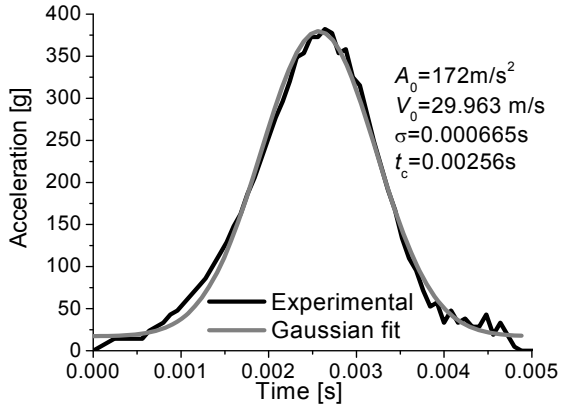

Fig. 4 – Drop test from 1.5m for hard material.

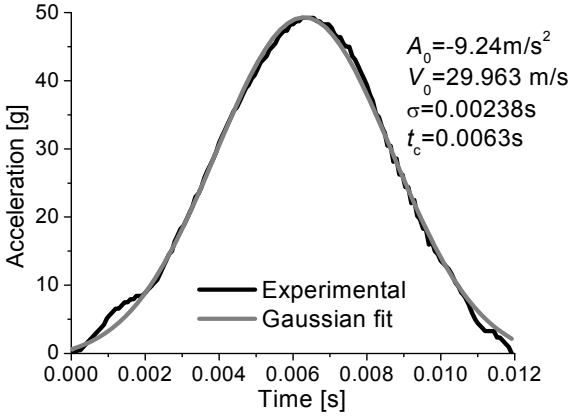

Fig. 5 – Drop test from 1.5m for soft material.

In this paper will be considered for shock acceleration input $\ddot{x}_0(t)$ the analytical expressions (9) for Gaussian (G) model with zero offset ($A_0 = 0$):

$$\ddot{x}_0(t) = \frac{V_0}{\sigma\sqrt{2\pi}} \exp\left[-\frac{(t-t_c)^2}{2\sigma^2}\right]. \tag{10}$$

The pulse width Δt, centered at time t_c is practically obtained when

$$\int_{t_c-\Delta t/2}^{t_c+\Delta t/2} \ddot{x}_0(\tau)\,d\tau = V_0 \int_{t_c-\Delta t/2}^{t_c+\Delta t/2} p(t;t_c,\sigma)d\tau = V_0\left[F\left(t_c+\Delta t/2;t_c,\sigma\right)-F\left(t_c-\Delta t/2;t_c,\sigma\right)\right] \cong V_0, \tag{11}$$

where $F(t;t_c,\sigma)$ is the Gaussian distribution function. From Chebyshev's inequality, results that for numerical simulation one must choose for the initial pulse time $t_0 \le t_c - 3\sigma$ such as the approximation (11) to be very accurate (less than $1\,\%_{00}$ error). Then, the value of parameter V_0 represents the magnitude of the initial shock velocity and $\Delta t = 6\sigma$ is the effective pulse width. The peak and average values of shock acceleration are given by

$$\ddot{x}_{0\max} = \frac{V_0}{\sigma\sqrt{2\pi}},\quad \ddot{x}_{0av} \cong \frac{1}{6\sigma}\int_{t_c-\Delta t/2}^{t_c+3\sigma} \ddot{x}_0(\tau)\,d\tau \cong \frac{V_0}{6\sigma}. \tag{12}$$

The time histories of shock acceleration, velocity and displacement, for $V_0 = 1\,\text{m/s}$, $\sigma = 0.01\,\text{s}$ and $t_c = 0.05\,\text{s}$ are shown in Fig. 6. As on can see from the acceleration time history, the values

$$\Delta t = 6\sigma = 0.06\,\text{s},\ \ddot{x}_{0\max} = \frac{V_0}{\sigma\sqrt{2\pi}} = \frac{1}{0.01\sqrt{2\pi}} \cong 39.9\,\text{m/s}^2,\ \ddot{x}_{0av} = \frac{V_0}{6\sigma} = \frac{1}{0.06} \cong 16.7\,\text{m/s}^2 \tag{13}$$

estimate very accurate the pulse width, the maximum and average shock acceleration. The shape of displacement time history can be viewed as the track profile for shock testing of road vehicles when the

riding speed is $V_1 = 1\,\mathrm{m/s}$. For an arbitrary value of vehicle speed V, the parameter σ from relation (10) should be replaced by $\sigma_V = (V_1/V)\sigma$.

In Figs. 7 and 8 are shown the time histories of shock acceleration $\ddot{x}_0(t)$ and their amplitude spectra for $V_0 = 1\,\mathrm{m/s}$ and different values of σ. The shapes of shock amplitude spectra are similar to amplitude–frequency characteristics of low-pass filters. Their cut-off frequencies, defined for –3dB attenuation, are shown in Fig. 8.

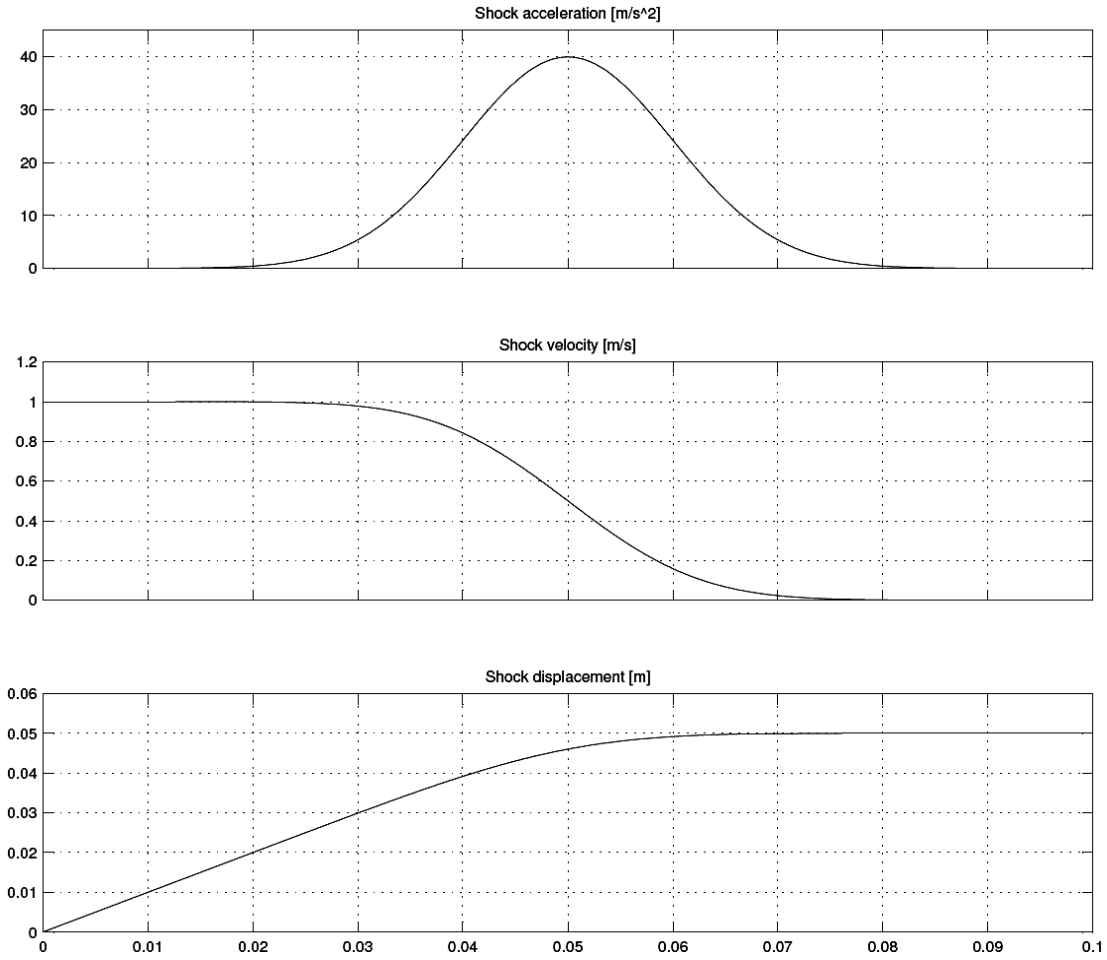

Fig. 6 – Time histories of shock acceleration, velocity and displacement.

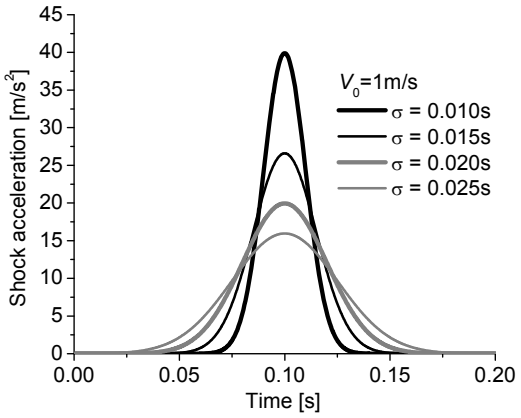

Fig. 7 – Time histories of shock accelerations.

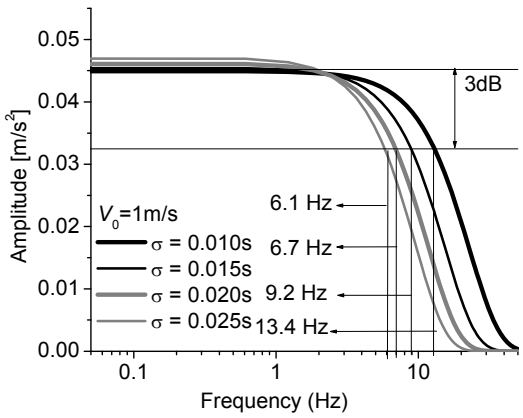

Fig. 8 – Amplitude spectra of shock accelerations.

4. ASSESSMENT OF DAMPERS CONDITION FOR LINEAR MODEL

For linear damping characteristics $f_i\left(y_i,\dot{y}_i\right)=c_i\dot{y}_i,\ i=1,2$ the system (3) can be written as:

$$\begin{cases}\ddot{y}_1=-2\zeta_1\omega_1\dot{y}_1-\omega_1^2y_1+2\mu\zeta_2\omega_2\dot{y}_2+\mu\omega_2^2y_2-\ddot{x}_0\\ \ddot{y}_2=2\zeta_1\omega_1\dot{y}_1+\omega_1^2y_1-2\left(1+\mu\right)\zeta_2\omega_2\dot{y}_2-\left(1+\mu\right)\omega_2^2y_2\end{cases},\tag{14}$$

where the damping ratios ζ_1 and ζ_2 are defined as:

$$\zeta_1=\frac{c_1}{2\sqrt{k_1m}}=\frac{c_1}{2m\omega_1},\ \zeta_2=\frac{c_2}{2\sqrt{k_2M}}=\frac{c_2}{2M\omega_2},\ \frac{c_2}{m}=\frac{c_2}{M}\frac{M}{m}=2\mu\zeta_2\omega_2.\tag{15}$$

The absolute accelerations $\ddot{x}_1=\ddot{y}_1+\ddot{x}_0$ and $\ddot{x}_2=\ddot{y}_2+\ddot{y}_1+\ddot{x}_0$ of sprung and unsprung masses of vehicle are obtained by numerical integration of system (14). The obtained results will be used to assess the suspension damper condition based on changes in system dynamic interactions between these two accelerations produced by the modification of damping ratio ζ_2. The equivalent linear damping ratio ζ_1 of tire hysteretic damping is usually very small and in many studies of vehicle suspensions based on quarter car model is neglected. Nevertheless, in the present study a variation interval $0\le\zeta_1\le0.1$ is considered for this coefficient. Also, the tire stiffness is prone to some variations around the nominal value k_1 ($\pm10\%$) leading to a certain modification of frequency ω_1 ($\pm5\%$). The values of these parameters, which depend on tire temperature, pressure and dynamic loading, are difficult to be controlled during the shock tests and could possibly influence the assessment of suspension damper condition. It is shown that by appropriate filtering of measured acceleration signals $\ddot{x}_1\left(t\right)$ and $\ddot{x}_2\left(t\right)$, the evaluation of equivalent damping ratio of vehicle suspension ζ_2 is practically independent of the possible variation of ζ_1 and ω_1.

In this paper the change in system dynamic interactions, due to the modification of damping ratio ζ_2, is evaluated by a *damping efficiency index* $I_{\mathrm{d}}\left(\zeta_2\right)$, defined by the absolute value of covariance coefficient defined as

$$I_{\mathrm{d}}(\zeta_2)=\left|\frac{1}{T\sigma_{\ddot{x}_2}\sigma_{\ddot{x}_1}}\int_0^T\left(\ddot{x}_{2\mathrm{f}}\left(t\right)-\mu_{\ddot{x}_2}\right)\left(\ddot{x}_{1\mathrm{f}}\left(t\right)-\mu_{\ddot{x}_1}\right)\mathrm{d}t\right|,\tag{16}$$

where $\ddot{x}_{1\mathrm{f}}\left(t\right),\ddot{x}_{2\mathrm{f}}\left(t\right)$ are obtained by band-pass filtering of measured acceleration signals $\ddot{x}_1\left(t\right)$ and $\ddot{x}_2\left(t\right)$, T is the record length, and $\mu_{\ddot{x}_{i\mathrm{f}}},\sigma_{\ddot{x}_{i\mathrm{f}}}$, $i=1,2$ are the mean values and the variances of filtered signals. An octave band-pass filter with central frequency $f_{\mathrm{c}}=\omega_2/2\pi$ and bandwith $\Delta f\cong0.7f_c$ was used to evaluate the effect of modification of suspension damping ratio ζ_2 on the values of index $I_{\mathrm{d}}\left(\zeta_2\right)$. Figure 9 shows the time histories of unfiltered and filtered acceleration output of system (3), obtained for following values of shock input system and parameters

$$\begin{gathered}V_0=1\ \mathrm{m/s},\ \ \sigma=0.01\ \mathrm{s},0.02\ \mathrm{s},\ \ t_{\mathrm{c}}=0.05\ \mathrm{s}\\ \zeta_2=0.3,\ \zeta_1=0.05,\ \omega_2=6.28\ \mathrm{rad/s},\ \omega_1=62.8\ \mathrm{rad/s},\ \mu{=}10.\end{gathered}\tag{17}$$

The values of damping efficiency index $I_{\mathrm{d}}\left(\zeta_2\right)$ were calculated by using relation (16) for the following values of parameters of shock input and suspension system:

$$\begin{gathered}V_0=1\mathrm{m/s},\ \ \sigma=0.01\mathrm{s},0.02\ \mathrm{s},\ T=15\ \mathrm{s},\ t_{\mathrm{c}}=0.05\ \mathrm{s}\\ \zeta_1=0,0.05,\ 0.1,\ \ \omega_1=2\pi f_1,\ f_1=9.95,10,10.5\mathrm{Hz},\ \zeta_2=0.1,0.15,..,0.5,\ \mu=10\end{gathered}\tag{18}$$

In Fig. 10 is plotted the function $\zeta_2\left(\tilde{I}_\mathrm{d}\right)$, where $\tilde{I}_\mathrm{d} = 0.5\left(\tilde{I}_{\mathrm{d}1} + \tilde{I}_{\mathrm{d}2}\right)$, and its polynomial regression fit

$$\zeta_2\left(\tilde{I}_\mathrm{d}\right) = -1.41767 + 7.34322\,\tilde{I}_\mathrm{d} - 11.54665\,\tilde{I}_\mathrm{d}^2 + 7.07369\,\tilde{I}_\mathrm{d}^3. \tag{19}$$

The results presented in Table 1 show that the values of index I_d are sensitive to the variation of suspension damping ratio ζ_2 and are practically independent of the tire damping and elastic properties, as well as of the shock input shape, for reasonable variation of these parameters. Therefore, the damping efficiency damping index proposed in this paper can be used to assess the condition of vehicle suspension dampers by conducting shock tests. The condition of dampers can evaluated in terms of the suspension damping ratio ζ_2, obtained from relation (19) for the measured value of damping efficiency index I_d. Usually, the allowed percentage of damping efficiency attenuation with respect to the nominal value is specified in the data sheets provided by the manufacturer of tested dampers.

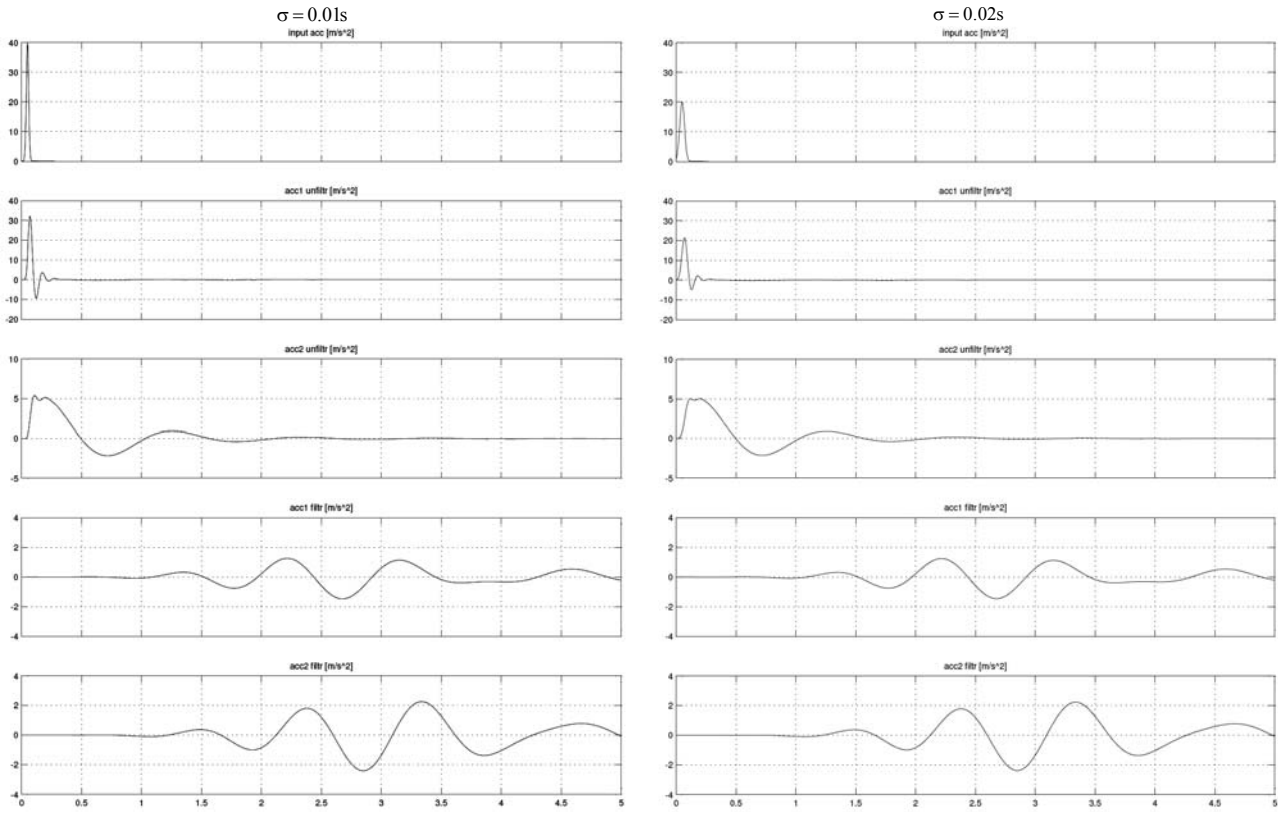

Fig. 9 – Unfiltered and filtered acceleration output for two different shock inputs.

Table 1

Values of damping efficiency index for different parameters of suspension system and shock input

ζ_1	0	0	0	0.05	0.05	0.05	0.1	0.1	0.1	σ	σ
f_1 [Hz]	9.95	10	10.05	9.95	10	10.05	9.95	10	10.05	0.01	0.02
ζ_2	I_d	I_d	I_d	I_d	I_d	I_d	I_d	I_d	I_d	$\tilde{I}_{\mathrm{d}1}$	$\tilde{I}_{\mathrm{d}2}$
0.1	0.407	0.405	0.403	0.408	0.406	0.404	0.408	0.406	0.404	0.406	0.407
0.15	0.418	0.417	0.415	0.416	0.417	0.416	0.419	0.418	0.417	0.417	0.419
0.2	0.454	0.453	0.452	0.453	0.453	0.453	0.455	0.454	0.453	0.453	0.455
0.25	0.498	0.498	0.497	0.498	0.498	0.498	0.500	0.499	0.498	0.498	0.500
0.3	0.545	0.545	0.544	0.545	0.545	0.545	0.546	0.546	0.546	0.545	0.547

Table 1 (continued)

0.35	0.591	0.590	0.590	0.591	0.591	0.591	0.592	0.591	0.591	0.591	0.592
0.4	0.633	0.633	0.633	0.633	0.633	0.633	0.634	0.634	0.633	0.633	0.634
0.45	0.671	0.671	0.671	0.671	0.671	0.671	0.672	0.672	0.672	0.671	0.673
0.5	0.705	0.705	0.705	0.706	0.706	0.706	0.706	0.706	0.706	0.706	0.706

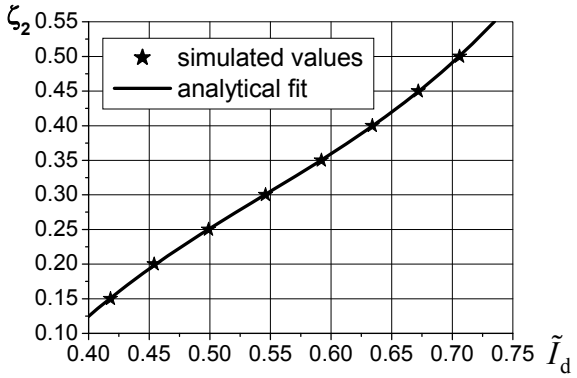

Fig. 10 – Variation of damping ratio ζ_2 vs. damping efficiency index $\tilde{I}_\mathrm{d}$.

5. ASSESSMENT OF DAMPERS CONDITION FOR NONLINEAR MODEL

In this case section the results obtained for linear case are used to assess the condition of viscous dampers with nonlinear damping characteristics modeled by relation (5). In view of relations (8) and (15) the expression of linear equivalent damping ratio coefficient $\zeta_{2\mathrm{e}}$ can be written as

$$\zeta_{2\mathrm{e}} = \frac{c_{2\mathrm{e}}}{2\omega_2 M} = \frac{a_2 \dot{y}_{\max}^{\alpha-1}}{2(\alpha+1)\omega_2 M} = \frac{2\lambda_2}{\alpha+1}, \quad \lambda_2 = \frac{a_2 \dot{y}_{\max}^{\alpha-1}}{2\omega_2 M}. \tag{20}$$

For a given values of exponent $\alpha > 0$, the variation of damping efficiency index $\tilde{I}_\mathrm{d}(\lambda_2)$, can be calculated by applying (16) to the filtered acceleration output of nonlinear system as in the case of linear damping. Obviously, $\zeta_{2\mathrm{e}} = \lambda_2$ for $\alpha = 1$. Then the results obtained in previous section for linear damping can be used to assess the maximum velocity $\dot{y}_{\max}(\zeta_2)$, such that the condition $\tilde{I}_\mathrm{d}(\lambda_2) = \tilde{I}_\mathrm{d}(\zeta_{2\mathrm{e}})$ is fulfilled with an imposed accuracy. Figures 11 and 12 illustrate the results of application the proposed algorithm to power law viscous damping characteristics, for $\alpha = 0.5$, $\alpha = 1$, $\alpha = 2$, and $\zeta_{2\mathrm{e}} = \lambda_2 \geq 0.2$.

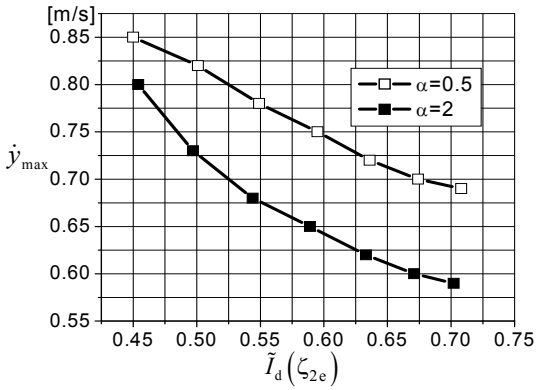

Fig.11 – Variation of maximum linearization velocity $\dot{y}_{\max}$ *versus* damping efficiency index $\tilde{I}_\mathrm{d}$.

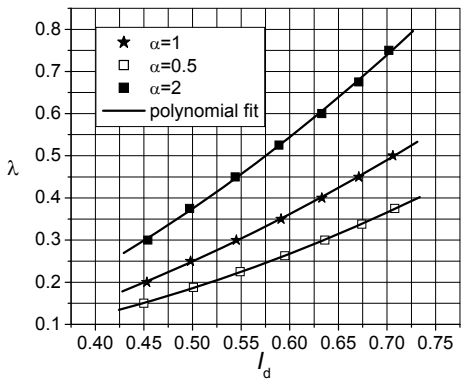

Fig. 12 – Variation of coefficients of linear and equivalent linear damping *versus* $\tilde{I}_\mathrm{d}$.

The expressions of analytical approximation by polynomial regression within considered interval for variation of damping efficiency index are

$$\begin{aligned}\zeta_2\left(\tilde{I}_\mathrm{d}\right) &= -0.07396+0.2507\,\tilde{I}_\mathrm{d}+0.79334\,\tilde{I}_\mathrm{d}^2, \text{ for } \alpha=1\\ \lambda_2\left(\tilde{I}_\mathrm{d}\right) &= 0.01705-0.06925\,\tilde{I}_\mathrm{d}+0.80075\,\tilde{I}_\mathrm{d}^2, \text{ for } \alpha=0.5\\ \lambda_2\left(\tilde{I}_\mathrm{d}\right) &= -0.0978+0.31545\,\tilde{I}_\mathrm{d}+1.25808\,\tilde{I}_\mathrm{d}^2, \text{ for } \alpha=2.\end{aligned} \tag{21}$$

6. CONCLUSIONS

In this paper is proposed a simple, effective and low cost method to assess the condition of suspension dampers for road vehicles and airplane landing gears. The method is based on the measurement of vertical accelerations on sprung and unsprung masses for a shock input applied at the road/runway-tire contact surface. For road vehicles the riding over a conveniently profiled bump can provide the desired shock acceleration input, while for airplanes this type of input is provided by the landing itself. By appropriate band-pass filtering of recorded signal a damping efficiency index is assessed. It is shown that this index depends only on the equivalent damping ratio of vehicle suspension, being practically independent of the tire damping and elastic properties, as well as of the peak value and duration of shock input, for reasonable variations of these parameters. The applicability of the proposed method is illustrated for linear and nonlinear viscous damping characteristics, using an equivalent linearization method based on equality of both dissipated powers per cycle and damping efficiency indices.

ACKNOWLEDGMENTS

The authors would like to express their gratitude to Romanian Academy and Polish Academy of Sciences for supporting this work through the inter-academic collaboration program.

REFERENCES

1. SIRETEANU T., GUNDISCH O., PARAIAN S., *Random Vibrations of Automobiles* (in Romanian), Edit. Tehnică, Bucharest, 1981.
2. GUGLIELMINO, E**.,** SIRETEANU, T., STAMMERS, C.W., GHITA, G., GIUCLEA, M. *Semi-active Suspension Control; Improved Vehicle Ride and Road Friendliness*, Springer, 2008.
3. PING LI, GOODALL R., *Model-based condition monitoring for railway vehicle systems*, Control 2004, University of Bath, UK, September 2004, ID-058.
4. MEI T. X., DING X. J., A model-less technique for the fault detection of rail vehicle suspensions, Vehicle System Dynamics,. **46**, 2008, p. 277-287.
5. MEI T. X., DING X. J., Condition monitoring of rail vehicle suspensions based on changes in system dynamic interactions, Vehicle System Dynamics, **47**, 9, 2009, p. 1167-1181.
6. WEI X., JIA L., LIU H., *Data-driven fault detection of vertical rail vehicle suspension systems*, UKACC International Conference on Control 2012, Cardiff, UK, p. 589-594.
7. KOJIMA T., SUGAHARA Y., *Fault detection of vertical dampers of railway vehicle based on phase difference of vibrations*, Quarterly Report of Railway Technical Research Institute, **54**, *3*, 2013, p. 139-144.
8. XIUKUN WEI , LIMIN JIA , HAI LIU, *A comparative study on fault detection methods of rail vehicle suspension systems based on acceleration measurements*, Vehicle System Dynamics, International Journal of Vehicle Mechanics and Mobility, **51**, *5*, 2013, p. 700-720.
9. MELNIK R., KOZIAK S., Rail vehicle suspension condition monitoring–approach and implementation, Journal of Vibroengineering, **19**, 1, 2017, p. 487-501.
10. SIRETEANU T., ANA-MARIA MITU, GHITA GHE., *Assessment the Condition Vehicle Dampers Based on Vibration Measurements*, ICMSAV&COMEC&eMEC 2018, Braşov, Romania, 25-26 October, pp. 57-64.
11. NICULESCU A.I., JANKOWSKI A., KOWALSKI M., SIRETEANU T., *Advantages conferred by shock absorbers with cylindrical actuator application to landing gear*, Journal of KONES Powertrain and Transport, **23**, *1*, 2016
12. KONIECZNY L, *Analysis of Simplifications Applied in Vibration Damping*, Shock and Vibration, Volume **2016**, Article ID 6182847.
13. CUI Y., THOAS R. KURFESS T.R., MESSMAN M., *Testing and modeling of nonlinear properties of shock absorbers for vehicle dynamics studies*, Proceedings of the World Congress on Engineering and Computer Science 2010, Vol. **II** – WCECS 2010, October 20-22, 2010, San Francisco, USA.

Received July 12, 2018